Molecular Crystals and Liquid Crystals

ISSN: 1056-8816 (Print) (Online) Journal homepage: http://www.tandfonline.com/loi/gmcl18

Measurements of Third Order Optical Nonlinearities of Nematic Liquid Crystals

P. Palffy-muhoray , H. J. Yuan , L. Li , Michael A. Lee , J. R. Desalvo , T. H. Wei , M. Sheik-bahae , D. J. Hagan & E. W. Van Stryland

To cite this article: P. Palffy-muhoray , H. J. Yuan , L. Li , Michael A. Lee , J. R. Desalvo , T. H. Wei , M. Sheik-bahae , D. J. Hagan & E. W. Van Stryland (1991) Measurements of Third Order Optical Nonlinearities of Nematic Liquid Crystals, Molecular Crystals and Liquid Crystals, 207:1, 291-305, DOI: 10.1080/10587259108032107

To link to this article: http://dx.doi.org/10.1080/10587259108032107

Mol. Cryst. Liq. Cryst., 1991, Vol. 207, pp. 291–305
Reprints available directly from the publisher
Photocopying permitted by license only

Printed in the United States of America

MEASUREMENTS OF THIRD ORDER OPTICAL NONLINEARITIES OF NEMATIC LIQUID CRYSTALS

P. Palffy-Muhoray, H.J. Yuan, L. Li and Michael A. Lee
Liquid Crystal Institute
Kent State University
Kent, OH 44242, USA

and

J.R. DeSalvo, T.H. Wei, M. Sheik-Bahae, D.J. Hagan, and E.W. Van Stryland
CREOL
University of Central Florida
Orlando, FL 32826, USA

ABSTRACT

In order to better understand the physical mechanisms responsible for the large observed optical nonlinearities of nematic liquid crystals, we have carried out nonlinear absorption and nonlinear refraction measurements on the pure liquid crystals 5CB and 8CB, and the liquid crystal mixture E7 using picosecond, nanosecond and millisecond pulses. We have used the recently developed Z-scan method[1-2], a sensitive single-beam technique which allows the determination of the sign and magnitude of the nonlinear refraction and the magnitude of the nonlinear absorption for aligned samples[3]. We have performed these measurements on aligned samples at wavelengths of 514nm and 532nm. In addition, we have studied the temperature dependence of the nonlinear refractive indices. Possible mechanisms responsible for the observed nonlinearities are discussed.

1. INTRODUCTION

The nonlinear optical response of liquid crystals has become the subject of increased study in recent years[4-7]. A large variety of mechanisms ranging from collective reorientation to electronic hyperpolarizability can contribute to the optical nonlinearities in these materials. We have carried out measurements of third order responses of the liquid crystals 5CB (4-cyano-4'-*n*-pentybiphenyl), 8CB (4-cyano-4'-*n*-octylbiphenyl) and E7 (a commercial mixture of biphenyls and terphenyls). In order to better understand the mechanisms contributing to the observed nonlinearities, we used geometries where director reorientation is not expected to occur, and we measured the nonlinearities on timescales ranging from milliseconds to picoseconds.

Several techniques have been developed in the past to measure the nonlinear refractive index n_2, or, equivalently, the real part of the third order susceptibility $\chi^{(3)}$. These include nonlinear interferometry[8], wave mixing[9,10], and beam-distortion measurements[11]. Interferometry and wave mixing are potentially sensitive techniques, but require relatively complex experimental arrangements. Beam-distortion measurements, on the other hand, require precise beam scans followed by complex wave-propagation analyses. We find that the single-beam Z-scan technique[1,2] is attractive because of its simplicity and sensitivity in measuring both the nonlinear refraction and nonlinear absorption. This technique is based on the transformation of phase distortion induced by the nonlinear medium to amplitude distortion during beam propagation.

In this paper, we report our measurements using the Z-scan technique of the intensity dependent third order nonlinearities of the pure liquid crystals 5CB and 8CB and the mixture E7 using nanosecond and picosecond pulses from frequency doubled Nd:YAG lasers and millisecond pulses from a CW Ar^+ laser. Both the nonlinear refractive indices and nonlinear absorption coefficients for light polarized parallel (denoted by the subscript $\|$) and perpendicular (denoted by $\perp$) to the director have been measured.

2. Z-SCAN TECHNIQUE

The schematic of the setup for the Z-scan experiment is shown in Fig. 1. A Gaussian laser beam is focused at z=0 plane, and the transmittance of a nonlinear medium through a finite aperture at $z=+d_0$ (where d_0 is the distance from focus to aperture) is measured in the far field as a function of the sample position z.

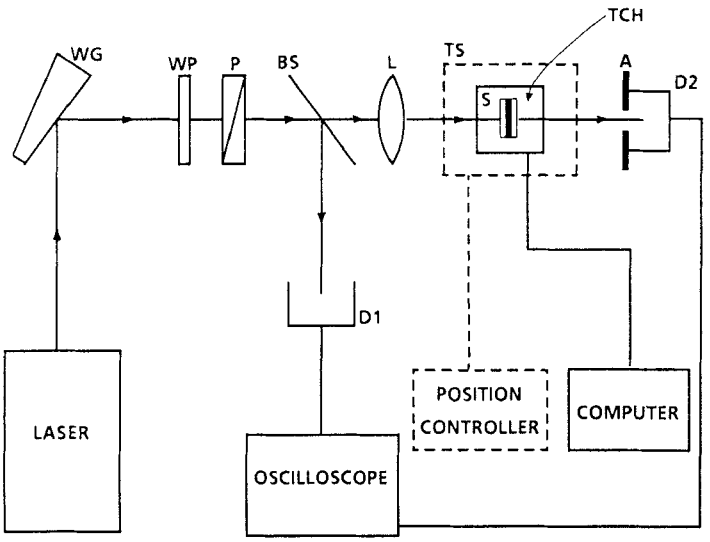

Fig. 1. Schematic of experimental setup for Z-scan measurements. The abbreviations are: WG, wedged glass; WP, wave plate; P, polarizer; BS, beam splitter; L, lens; TS, translation stage; S, liquid crystal sample; TCH, temperature controlled housing; A, aperture; D1 and D2, photodiode detectors.

The following example illustrates the Z-scan method. A thin sample, with thickness smaller than the diffraction length of the focused beam, with a positive nonlinear refractive index n_2 can be regarded as a thin converging lens,

whose focal length varies with intensity; that is, with sample position along the z-axis. Starting the scan far from the focal point at large negative values of z, the beam intensity is low and nonlinear effects are negligible. Initially, therefore, the transmittance remains essentially constant. As the sample is moved closer to the focus, the beam intensity increases significantly, leading to a self-focusing in the sample. This self-focusing with the sample positioned at small negative values of z will cause the beam to broaden at the aperture, decreasing the measured transmittance. As the sample is moved through the focus to a post-focal position, the same self-focusing causes the beam to narrow at the aperture, increasing the transmittance. Consequently a pre-focal minimum (valley) followed by a post-focal maximum (peak) in the transmittance versus sample position curve corresponds to a positive n_2; and conversely a peak followed by a valley is a signature of a negative n_2. The magnitude of n_2 can be evaluated using the analysis presented in Refs. 1 and 2.

In addition, the nonlinear absorption can be determined by performing a Z-scan with the aperture removed (open aperture Z-scan). The transmittance in this case is independent of the effects of nonlinear refraction, so that the change in transmittance gives a measure of the nonlinear absorption.

While a complete analysis is given in Refs. 1 and 2, an estimate of both the nonlinear absorption coefficient β and the nonlinear refractive index n_2 can be made as follows. For an open aperture Z-scan, the total change in transmittance ΔT_{abs} in moving the sample from a position far from focus (z > diffraction length) to focus (z=0) is

$$\Delta T_{abs} \simeq -\frac{\beta}{2\sqrt{2}} I_o(1-R) L_{eff} \qquad (1)$$

where $L_{eff}= (1-e^{-\alpha L})/\alpha$ and α is the linear absorption coefficient, L is the sample thickness, I_o is the on axis intensity at focus, and R is the surface reflectivity.

For a purely refractive nonlinearity, as shown in Ref. 2, the change in transmittance from peak to valley ΔT_{p-v} is linear in the (time averaged) phase distortion on axis at focus. For a finite aperture, this is given by

$$\Delta T_{p-v} \simeq 0.406(1- A)^{0.25} < \Delta\Phi_o > \quad (2)$$

where A is the linear transmittance of the aperture, and the phase distortion $<\Phi_o>$ is

$$<\Phi_o> = \frac{2\pi}{\lambda} < \Delta n_o > L_{eff}. \quad (3)$$

The on axis index change at focus is related to the nonlinear refractive index n_2 and γ by

$$<\Delta n_o> = < \frac{n_2}{2} |E_o|^2 > = < \gamma I_o > \quad (4)$$

where E_o is the peak electric field on axis at focus.

In the case where nonlinear absorption is taking place simultaneously with nonlinear refraction, the nonlinear absorption coefficient β can be determined from an open aperture Z-scan. With β known, a finite aperture (A<1) Z-scan can be performed to determine the nonlinear refractive index γ or n_2. Detailed calculations show[1] that for a material with $\beta/2k|\gamma| \leq 1$, there exists a simple procedure to calculate γ with less than 10% error. The process is simply to divide the normalized finite aperture (A<1) transmittance by the normalized open aperture one (A=1); the new transmittance curve thus obtained can then be used to calculate n_2 as if β=0.

3. EXPERIMENTAL RESULTS

The pure liquid crystals 5CB and 8CB, and the mixture E7 obtained from EMI Chemicals were used without further purification. The nematic-isotropic transition temperatures of 5CB, 8CB and E7 are 35.3°C, 40.5°C and 60°C,

respectively, and 8CB also exhibits a nematic - smectic A transition at 33.5°C. The liquid crystal samples were sandwiched between two 25mm x 38mm x 0.9mm glass plates. The plates were either coated with PVF (polyvinyl formal) and then buffed to achieve homogeneous (planar) alignment (HGA), or coated with silane for homeotropic alignment (HTA). The glass plates were separated by 25μm and 120μm mylar spacers. The experimental setup is shown in Fig. 1. We used frequency doubled Nd:YAG lasers, one with T_{FWHM} = 33ps and the other with T_{FWHM} = 7ns Gaussian pulses, and a CW Ar^+ laser with a shutter providing 10ms square pulses for our measurements. A wave plate and polarizer combination was used to control the pulse energy, which was selected to optimize the Z-scan measurements. In the millisecond and nanosecond measurements, the temporal pulse profile was monitored using a fast photodiode D1, and the transmittance after the aperture was measured by detector D2. A converging lens (f=125mm) was used to focus the Gaussian beam to a beam waist ($HWe^{-2}M$) of w_0=14.5μm in the millisecond case, w_0=7.5μm in the nanosecond case, and of w_0=18.9μm in the picosecond case. The liquid crystal samples were mounted in an Instec temperature controlled housing (TCH) whose temperature was computer controlled. A Daedal translation stage (TS) was used to position the sample with $\pm 1\mu$m resolution.

Fig. 2 shows the Z-scans (normalized transmittance as function of sample position z) of an 120μm thick homogeneously aligned 5CB sample for the $E \perp \hat{n}$ geometry. T_{FWHM} = 33ps pulses from a frequency doubled Nd:YAG laser with peak on-axis laser intensity I_0 = 23.3 GW/cm^2 were used in this measurement. The symbols □ show the normalized transmittance with a 40% aperture before detector D2. The valley-peak configuration indicates self-focusing, while the strongly suppressed peak indicates strong nonlinear absorption occuring simultaneously with the nonlinear refraction. Measured transmittances from an open aperture Z-scan are shown with the symbol × in Fig. 2. From this data we obtain the nonlinear absorption coefficient $\beta_\perp$(HGA) = 0.78 cm/GW. After removing the contribution of nonlinear absorption by dividing the finite (40% in this case) aperture transmittance by the open aperture transmittance, the antisymmetric shape of the curve is recovered. The results of the divison are shown in Fig.3 with the symbol +. The nonlinear refractive index obtained by analysing the results of these measurements is $n_{2\perp}$(HGA) = $+6.9\times10^{-12}$ esu.

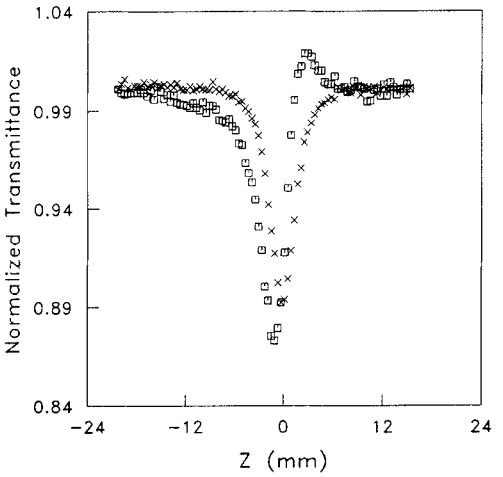

Fig. 2. Transmittance of a planar aligned 120μm thick 5CB sample in $\hat{n} \perp E$ geometry using 33 ps laser pulses from a frequency doubled Nd:YAG laser. □ represents trasmittance with 40% aperture; × represents transmittance with open aperture. The peak on-axis laser intensity was $I_0 = 23.3$ GW/cm^2.

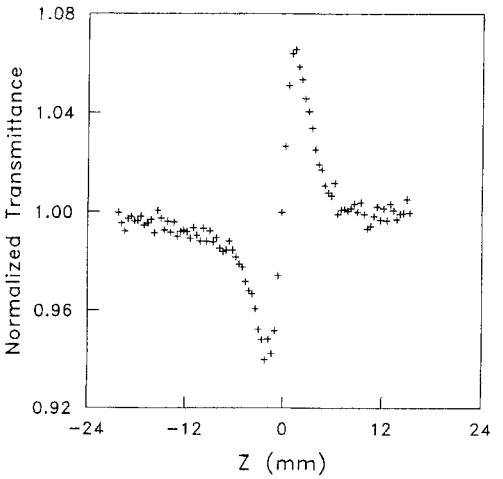

Fig. 3. Transmittance obtained by dividing the small aperture transmittance data by the open aperture transmittance of Fig.2.

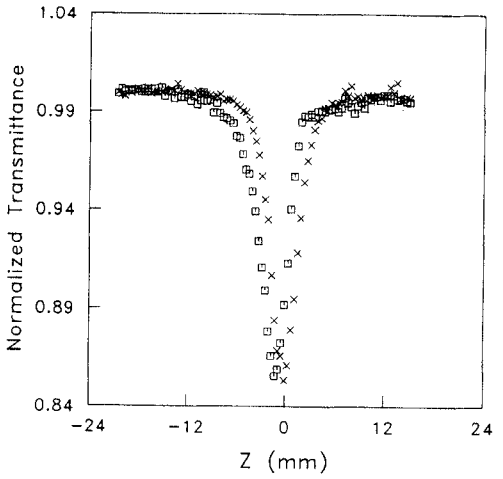

Fig. 4. Transmittance of a planar aligned 120μm thick 5CB sample in $\hat{n}||E$ geometry using 33 ps laser pulses from a freequency doubled Nd:YAG laser. □ represents transmittance with 40% aperture; × represents transmittance with open aperture. The peak on-axis laser intensity was $I_0 = 8.33$ GW/cm^2.

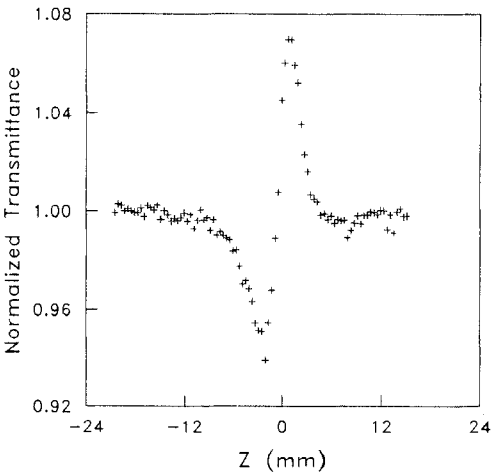

Fig. 5. Transmittance obtained by dividing the small aperture transmittance data by the open aperture transmittance of Fig.4.

Fig.4 shows measurements for the same planar sample but with the $E\|\hat{n}$ geometry. The pulse duration T_{FWHM} = 33ps is the same, but here the peak on-axis laser intensity is I_0 = 8.33 GW/cm^2. The symbols used are the same as in Fig. 2, with □ for the 40% aperture measurements and × for the open aperture measurements. From the open aperture measurements we obtain $\beta_{\|}$(HGA) = 2.27 cm/GW. The data, after removing the nonlinear absorption effects, is shown in Fig.5 and the nonlinear refractive index in this geometry is $n_{2\|}$(HGA) = 1.04×10^{-11} esu.

Fig. 6 shows the results of measurements on a 120μm thick homeotropically aligned 5CB sample with T_{FWHM} = 33ps pulses from the frequency doubled Nd:YAG laser with peak on-axis laser intensity I_0 = 23.3 GW/cm^2. In this case , the electric field E of the laser beam is perpendicular to the nematic director $\hat{n}$. The open aperture measurements are shown with the symbol ×, and the 40% aperture measurements are shown in with the symbol □. The nonlinear absorption coefficient is $\beta_{\perp}$(HTA) = 0.81 cm/GW.

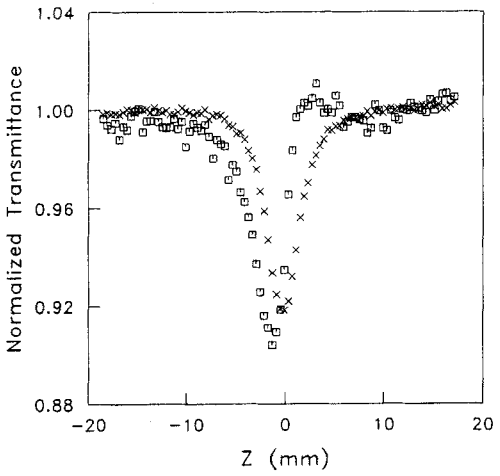

Fig. 6. Transmittance of a homeotropically aligned 120μm thich 5CB sample ($\hat{n} \perp E$) using 33 ps laser pulses from a frequency doubled Nd:YAG laser. □ represents transmittance with 40% aperture; and × represents transmittance with open aperture. The peak on-axis laser intensity was I_0 = 23.3 GW/cm^2.

The results after division are shown in Fig.7, and the nonlinear refractive index is $n_{2\perp}(\text{HTA}) = 5.7\times10^{-12}$ esu.

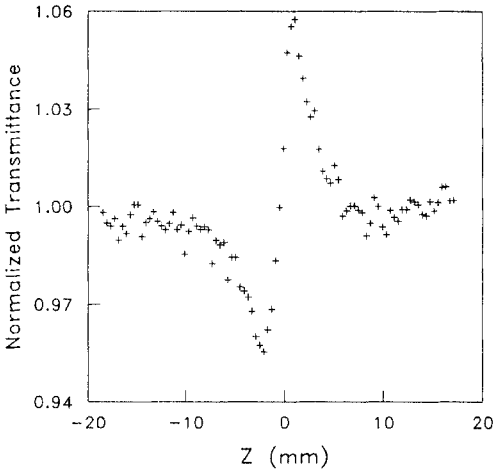

Fig. 7. Transmittance obtained by dividing the small aperture transmittance data by the open aperture transmittance of Fig.6.

We have also carried out measurements on the 25μm thick planar aligned 5CB sample in both $\hat{n}\perp E$ and $\hat{n}\|E$ geometries with T_{FWHM} = 6.5ns Gaussian pulses from a frequency-doubled Nd:YAG laser and 10 ms square pulses from a CW Ar^+ laser. Fig.8 shows the nanosecond results measured at T=25.0 °C in the $\hat{n}\|E$ geometry for a 1% aperture after division by nonlinear absorption (open aperture) data. The peak-valley configuration of the data shows a strong self-defocusing process and the nonlinear coefficients are $\beta_{\|}(\text{HGA}) = 265$ cm/GW and $n_{2\|}(\text{HGA}) = -1.75\times10^{-9}$ esu. The measurements for the same sample for $\hat{n}\perp E$ geometry give $\beta_{\perp}(\text{HGA}) = 36$ cm/GW and $n_{2\perp}(\text{HGA}) = +0.25\times10^{-9}$ esu. The same results were obtained from 120μm thick samples.

In the 10 ms measurements, the nonlinear refractive indices obtained at T=24 °C are $n_{2\|}(\text{HGA}) = -1.30\times10^{-3}$ esu and $n_{2\perp}(\text{HGA}) = +0.26\times10^{-3}$ esu. Fig.9 shows the temperature dependence of the measured nonlinear refractive indices for both parallel and perpendicular geometries. These results are qualitatively consistent with laser heating of the sample and the consequent reduction of orientational order.

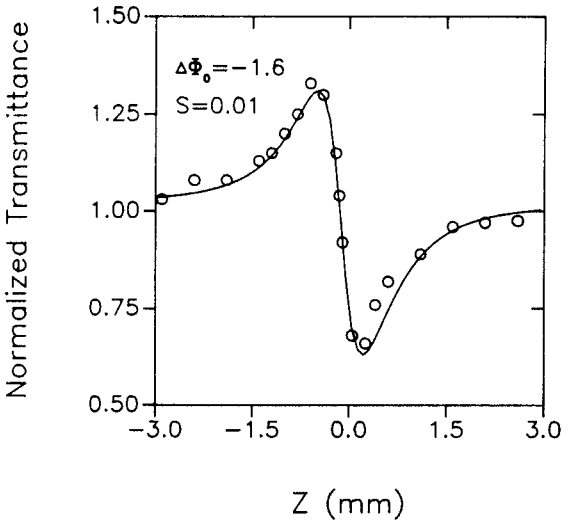

Fig. 8. Transmittance obtained by dividing the small aperture transmittance data by those obtained with open aperture. 7 ns pulses were used from a frequency doubled Nd:YAG laser. Open circles are results of division, and the solid line is the theoretical fit.

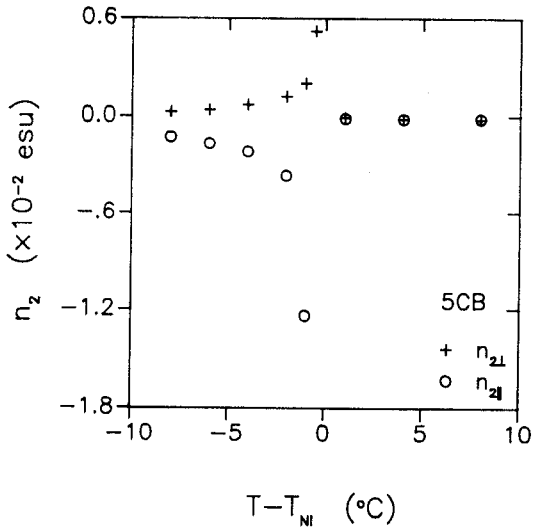

Fig. 9. The temperature dependence of $n_{2\parallel}$ and $n_{2\perp}$ for the nematic liquid crystal 5CB using 10ms Ar^+ laser pulses at $\lambda=514$ nm. The nonlinear birefringence diverges as $(T_{NI}-T)^{-1}$.

The nonlinear birefringence approximately follows the power law $(n_{2\perp} - n_{2||}) \propto (T_{NI} - T)^{-1}$ for temperatures below the nematic to isotropic transition temperature T_{NI}. If the linear absorption and laser heating of the sample are independent of polarization, then one would expect the relation $n_{2||} \simeq -2\, n_{2\perp}$ to hold[7]. Deviations from this relation in our results are likely due to dichroism of our sample. In this regime (10ms Ar^+ pulses) we did not observe nonlinear absorption within the sensitivity of our experiment.

The measured nonlinear refractive indices and nonlinear absorption coefficients for the liquid crystals 5CB, 8CB and E7 at T=24 °C and λ=532 nm with T_{FWHM}=6.5 ns pulses from a Q-swithed Nd:YAG laser are summarized in Table I. The results are compared with the nonlinear refractive indices of CS_2. For polarization parallel to the nematic director, the nonlinearities of these liquid crystals are two orders of magnitude larger than that of CS_2. For polarization perpendicular to the nematic director, the nonlinearities are one order of magnitude larger than that of CS_2.

Table I. Nonlinear refractive indices and nonlinear absorption coefficients for sample materials* at 24°C. T_{FWHM} = 6.5ns, λ = 532nm.

material	CS_2	5CB	8CB	E7
$n_{2||}$ ($\times 10^{-11}$esu)	+1.2	−175	− 77	−115
$n_{2\perp}$ ($\times 10^{-11}$esu)	+1.2	+ 25	+ 11	+ 10
$\beta_{||}$ (cm/GW)		265	246	284
$\beta_{\perp}$ (cm/GW)		36	20	40

*homogeneously aligned liquid crystal samples

The nonlinear refractive indices and absorption coefficients measured for liquid crystal 5CB at T=24 °C with different pulse durations are summarized in Table II. It is interesting to note that $n_{2||}$ changes sign from negative to positive as the pulse duration is changed from nano- to picoseconds indicating a change in the physical response.

Table II. Nonlinear refractive indices and nonlinear absorption coefficients for homogeneously aligned 5CB at 24°C.

T_{FWHM} (s)	10×10^{-2}	6.5×10^{-9}	33×10^{-12}
λ (nm)	514	532	532
$n_{2\|\|}$ (esu)	-1.30×10^{-3}	-1.75×10^{-9}	$+1.04 \times 10^{-11}$
$n_{2\perp}$ (esu)	$+0.26 \times 10^{-3}$	$+0.25 \times 10^{-9}$	$+0.69 \times 10^{-11}$
$\beta_{\|\|}$ (cm/GW)		265	2.27
$\beta_{\perp}$ (cm/GW)		36	0.78

4. DISCUSSION AND CONCLUSIONS

All measurements reported in this paper were carried out using a single laser pulse at each sample position. Using 33 ps pulses at λ=532 nm, we measured both nonlinear refractive indices and absorption coefficients for nematic liquid crystal 5CB in both $\hat{n} \perp E$ and $\hat{n} || E$ geometries using the Z-scan technique. For both polarizations we observed self-focusing. Electronic effects likely dominate in these picosecond measurements, although optical field induced changes in the orientational order could also contribute. Calculations to estimate the extent of this contribution are currently under way. The population of excited states may also contribute to the nonlinear response. If fast electronic effects dominate, then it may be possible to relate the measured anisotropies of both n_2 and β to the results of molecular hyperpolarizability calculations.

In the 10 ms pulse measurements at λ=514 nm we have observed strong nonlinear refraction and nonlinear birefringence. Self defocusing occurs in the $E||\hat{n}$ geometry where the polarization is parallel to the director, and self focusing in the $E \perp \hat{n}$ geometry. The nonlinear birefringence is strongly temperature dependent with $\Delta n_2 = n_{2\perp} - n_{2||} \approx 1.4 \times 10^{-2}$ $(T_{NI} - T)^{-1}$ esu·K. In our geometry, director reorientation is not expected to occur because there is no

torque exerted on the director by the optical field with $E||\hat{n}$; and because the threshold for optical twist transition[11] in the $E\perp\hat{n}$ configuration is well above the intensities used in this experiment. We expect theorefore that the observed nonlinearity is mainly due to laser heating of the sample. Such heating would result in changes in the orientational order parameter, the density, and consequently the refractive indices. A crude estimate of the magnitude of the thermally induced nonlinearity[7] is consistent with our measured values. However, preliminary measurements of the temporal profile of the outgoing pulse suggest that the response time of the process is longer than the estimated thermal diffusion time. The reason for this discepancy is not understood at this time.

In the measurements using 7 ns pulses at λ=532 nm, we observed strong nonlinear refraction, birefringence and nonlinear absorption. The mechanisms which give rise to these large nonlinearities and large anisotropy are not well understood. It might be expected that one important contribution is again laser heating of the sample. The measured values are six orders of magnitude smaller than the millisecond results, which is comparable to the expected contribution[7] from thermal effects with millisecond response times. However, preliminary pulse profile measurements indicate that this is a fast process, on the nanosecond scale. In addition, the large nonlinear absorption observed here, but not in the millisecond regime, suggest that excited state absorption rather than laser heating may be the responsible mechanism.

The third order nonlinearities in the liquid crystals studied with nanosecond pulses are two orders of magnitude larger than that of CS_2. The large nonlinear refractive index and nonlinear birefringence of these materials may be useful for device applications.

5. ACKNOWLEDGEMENTS

This work was supported by DARPA through US Army CECOM Center for Night Vision and Electro-Optics. E. W. Van Stryland also wishes to thank ARO/UASVAL for support. We acknowledge useful discussions with J. Kelly of the Liquid Crystal Institute at Kent State University and M. J. Soileau of CREOL at the University of Central Florida.

REFERENCES

1. M. Sheik-Bahae, A.A. Said and E.W. Van Stryland, Opt. Lett. 14, 955 (1989).
2. M. Sheik-Bahae, A.A. Said, T.H. Wei, D.J. Hagan, E.W. Van Stryland, *IEEE J. Quantum Electron.* QE-26, 760 (1990).
3. H.J. Yuan, L. Li and P. Palffy-Muhoray, SPIE Proc. 1307 (1990).
4. N.V. Tabiryan, A.V. Sukhov and B.Ya. Zel'dovich, *Mol. Cryst. Liq. Cryst.* Special Topics XIX, 136, 1,(1986).
5. I.C. Khoo, in *'Progress in Optics, XXVI'*, ed. E. Wolf (North Holland, New York, 1988).
6. I. Janossy, in *'Perspectives in Condensed Matter Physics'*, ed. L. Miglio, (Kluwer Academic Publisher, 1990).
7. P. Palffy-Muhoray, in *'Liquid Crystals - Applications and Uses'*, ed. B. Bahadur, (World Scientific, Singapore, 1990).
8. M.J. Weber, D. Milam, and W.L. Smith, Opt. Eng.17, 463 (1978).
9. S.R. Friberg and P.W. Smith, IEEE J. Quantum Electron. QE-23, 2089 (1987).
10. P.A. Madden, F.C. Saunders and A.M. Scott, IEEE J. Quantum Electron. QE-22, 1287 (1986).
11. W.E. Williams, M.J. Soileau, and E.W. Van Stryland, Opt. comm. 50, 256 (1984).
12. E. Santamato, G. Abbate and P. Maddalena, Phys. Rev. A 36, 2389 (1987).